RESEARCH ARTICLE | MARCH 15 1987

The Hückel model for small metal clusters. I. Geometry, stability, and relationship to graph theory

Youqi Wang; Thomas F. George; D. M. Lindsay; A. C. Beri

J. Chem. Phys. 86, 3493–3499 (1987)
https://doi.org/10.1063/1.452005

The Hückel model for small metal clusters. I. Geometry, stability, and relationship to graph theory

Youqi Wang[a] and Thomas F. George
Department of Chemistry and Department of Physics and Astronomy, State University of New York at Buffalo, Buffalo, New York 14260

D. M. Lindsay
Department of Chemistry, City College of the City University of New York, New York, New York 10031

A. C. Beri
Computer Sciences Corporation, Beltsville, Maryland 20705

(Received 23 May 1986; accepted 3 December 1986)

The relative stabilities of alkali-like metal clusters, M_n and M_n^+ with $2 \leqslant n \leqslant 9$, are calculated within the framework of the simple Hückel model. With the aid of graph theory, the binding energies for *all possible* Hückel structures are determined. With the exception of M_5^+ and M_6^+, the Hückel model gives minimum energy structures which are the same as those predicted by recent local-spin-density and configuration interaction calculations. Since the Hückel method is independent of the mechanical details of the bonding, a close connection is inferred between a cluster's stability and its topology. In the paper following this one, the Hückel results are extended to include absolute atomization energies and ionization potentials. In addition, it is shown that cluster energies may be quantitatively extrapolated to the bulk phase.

I. INTRODUCTION

Perhaps the most fundamental problem in metal cluster research is the determination of cluster structures. Surprisingly, despite a considerable research effort and many elegant experiments, only in rare instances has progress in this direction been made. Thus, for the alkali metals, only the trimer and heptamer structures are known with any certainty.[1–5] Again for the Group IA elements, most experiments have been concerned with properties such as ionization potentials,[6–11] relative abundances[12,13] and dissociation energies,[14–17] which only indirectly probe the structure of the clusters themselves. Accordingly, the task of determining cluster structures has fallen largely to the theoreticians. Even here, however, the available information is relatively sparse, except (we exclude dimers) in the case of alkali trimers.[18–20] Notable, in that a range of cluster sizes and geometries were considered, are recent semiempirical[21] and near *ab initio*[22–27] calculations on alkali metal clusters containing up to eight atoms. A principal prediction of two of these studies[23–26,27] is a tendency for the smaller alkali metal clusters to adopt planar geometries. Only for the seven atom and larger clusters are *true* three-dimensional structures found.

In this paper, we present simple Hückel calculations for alkali-like metal clusters, M_n and M_n^+ with $n \leqslant 9$. Using graph theoretical methods, we are able to assess the relative stabilities of *all possible* bonding arrangements and so determine the most stable Hückel structures at each cluster size. Except for M_5^+ and M_6^+, the most stable neutral and cation structures are exactly the same as those predicted by the more rigorous *ab initio* techniques of Refs. 23–27 and those confirmed by experiments.[1–5]

[a] Present address: Department of Chemistry, California Institute of Technology, Pasadena, CA 91125.

II. HÜCKEL CALCULATIONS AND GRAPH THEORY

The Hückel Molecular Orbital (HMO) model[28–30] provides the simplest quantum mechanical description of molecular bonding. In its most elementary form, the Hückel problem reduces to one of finding the eigenvalues and eigenvectors of the Hückel matrix whose elements are taken to be

$$\langle i|H|i\rangle = H_{ii} = \alpha$$

$$\langle i|H|j\rangle = H_{ij} = \begin{cases} -\beta & \text{if } i \text{ is bonded to } j \\ 0 & \text{otherwise} \end{cases} \tag{1}$$

with $1 \leqslant i \neq j \leqslant n$. An explicit form for the Hamiltonian is not defined, and the Hückel Coulomb (α) and resonance ($\beta > 0$) parameters are generally chosen by comparison with experimental data. Likewise, no particular choice of atomic basis functions $|i\rangle$ need be made. For alkali metal clusters, as considered in this paper, the set of valence s-orbitals, one from each atom, is the implied basis.

For an n-atom neutral cluster, the molecular binding energy $E^0(n)$ is obtained using the Aufbau principle and

$$E^0(n) = n\alpha + \sum_i n_i \epsilon_i, \tag{2}$$

where

$$n = \sum_i n_i \tag{3}$$

with n_i as the electron occupancy of neutral cluster eigenvalue ϵ_i. Similarly, a singly charged cation cluster has a binding energy

$$E^+(n) = (n-1)\alpha + \sum_i n_i \epsilon_i^+ \tag{4}$$

with

$$(n-1) = \sum_i n_i. \tag{5}$$

 0021-9606/87/063493-07$02.10

It is most convenient to consider the dimensionless Hamiltonian

$$H_{ii} = 0$$
$$H_{ij} = \begin{cases} -1 & \text{if } i \text{ bonded to } j \\ 0 & \text{otherwise} \end{cases} \quad (6)$$

which is equivalent to Eq. (1) but with energies given in the units of β relative to $\alpha = 0$. We term energies expressed in this way as being in "Hückel units" (hu). Written in the form of Eq. (6), the Hückel matrix has now a one-to-one correspondence with the adjacency matrix A of a simple graph[31]

$$\mathrm{A}_{ii} = 0$$
$$\mathrm{A}_{ij} = \begin{cases} 1 & \text{if } i \text{ adjacent to } j \\ 0 & \text{otherwise} \end{cases} \quad (7)$$

which means that every Hückel structure has a corresponding simple graph if each atom represents a vertex or point (n) in the graph and each bond (q) between adjacent atoms represents a line or edge of the graph.[32]

Our purpose is to search for all possible Hückel structures for an n-atom cluster and find the eigenvalues for each structure, in order to determine the most stable ones according to Eqs. (2) and (4). Because of the relation mentioned above, we can thus convert our problem into a study of all graphs with n vertices. At first sight, this is a formidable task, since there is a total of $2^{n(n-1)/2}$ different adjacency matrices for an n-vertex graph. Thus, for example, it would require nearly 10^{11} diagonalizations in order to find the most stable structure for a nine-atom cluster. Fortunately, most of these structures are isomorphic, i.e., the graphs they represent differ from one another merely by different labelings of the vertices. The actual number of distinct (n,q) graphs which are also connected (i.e., the cluster has not dissociated) can be determined from Polya's enumeration theorem.[31,33] Table I gives these numbers for $n \leqslant 10$, obtained by using the counting polynomials given in Ref. 33. Thus, for example, only about 3×10^5 graphs need be considered for $n = 9$, which is practically executable.

The main difficulty now lies in recognizing and eliminating isomorphic graphs. To our knowledge, there is no efficient and foolproof algorithm for this process.[34] However, we notice that a simple graph may be described by its adjacency matrix or *equivalently* by its incidence matrix.[31,33] The latter is an $n \times q$ matrix whose rows are labeled (as in the case of the adjacency matrix) by the vertices of the graph, but the column labels pertain to the edges of the graph. The inherent advantage of describing a graph by its incidence matrix lies in the fact that any exchange of rows or columns of the matrix does not alter the graph it represents, and there is no interference between the exchanges of the rows and columns, making it possible to bring an incidence matrix into its "standard form" and allowing for an ease of comparison amongst possibly isomorphic graphs.

We define the standard incidence matrix for a particular (n,q) graph as the one in which the rows (i.e., vertices) are arranged in order of *decreasing "connectivity"* and the columns (i.e., edges) are in *optimized descending "sequence order."* We specify the connectivity of a vertex i in terms of its first, second, third, and (if necessary) higher-order degrees. The first-order degree D_i^1 is a scalar, which is simply the number of vertices connected to it and given by the sum of the entries (0 or 1) in row i of the incidence matrix. If for two vertices i and j, $D_i^1 > D_j^1$, we say that vertex i has higher connectivity than j. If two vertices have the same first-order degree, we check their connectivities using a second-order degree. For vertex i, this is defined as the vector

$$\mathbf{D}_i^2 = (D_{i1}^1, D_{i2}^1, \ldots, D_{ik}^1), \quad (8)$$

where $k = D_i^1$, $D_{ij}^1 \geqslant D_{ih}^1$ if $j < h$, and D_{ij}^1 are the first-order degrees of the vertices which connect to the vertex i. For two vertices i and j which have the same first-order connectivity, we determine their second-order connectivity by comparing (one by one) the elements D_{ih}^1 and D_{jh}^1 of $\mathbf{D}_i^2$ and $\mathbf{D}_j^2$. If at a particular h, $D_{ih}^1 > D_{jh}^1$ (for example), then we assign a higher connectivity to vertex i. If for all h, $D_{ih}^1 = D_{jh}^1$, then we have to check the third-order connectivity (which is a matrix), and so on.

Each of the $1 \leqslant i \leqslant q$ columns of a particular incidence matrix may be thought of as a binary number b_i, since each entry can only be either 0 or 1. Thus we can define the "sequence order" of an incidence matrix through the vector.

$$\mathbf{S}_q = (b_1, b_2, \ldots, b_q), \quad (9)$$

where $b_i > b_j$ for $i < j$. For a simple graph, no two b_i can have the same value. In fact, $\mathbf{S}_q$ is a compact form of the incidence matrix and contains the same amount of information as in the original $n \times q$ form. If all the vertices of a given graph have different connectivities, then there is a unique standard incidence matrix ($\mathbf{S}_q$). Equivalently, if two graphs have the same $\mathbf{S}_q$, they are isomorphic.[35]

In order to produce all possible graphs having n vertices, we start from the complete graph (n,q_0), $q_0 = n(n-1)/2$, i.e., one in which each vertex is connected to every other one. By removing edges (i.e., breaking bonds) one at a time, we can generate all the graphs, each with the same number of vertices but with progressively fewer bonds. Consider a set of m (n,q) graphs at some particular point in this chain and call them "parent graphs." By removing one edge from a parent graph, we generate an $(n,q-1)$ subgraph. Since there are q bonds in the parent graph, we can get q apparently different $(n,q-1)$ subgraphs where this set contains a total of $m \times q$ graphs, many of which are isomorphic. It is easy to recognize and reject the disconnected graphs, and by comparing each of the subgraphs with its standard incidence matrix, the isomorphic ones can also be canceled. The new set of graphs now forms a collection of parent graphs for the next bond-breaking step. This procedure is repeated until $q = n - 1$, since this is the minimum q for a connected n-vertex graph.

In practice, we determined the standard incidence matrices only up to their third-order connectivities. Thus our algorithm does not ensure that we eliminate *every* isomorphic graph. All surviving graphs were then diagonalized and the eigenvalues of the possibly isomorphic ones were compared. If two (or more) graphs were found to have the same set of eigenvalues *and* the same connectivity to the third order, a further inefficient but safe comparison was made. The adjacency matrices of these graphs were reordered by permuting their rows and columns. Two graphs which be-

TABLE I. Number of connected simple graphs with n vertices and q edges.

q/n	2	3	4	5	6	7	8	9	10
1	1								
2		1							
3		1	2						
4			2	3					
5			1	5	6				
6			1	5	13	11			
7				4	19	33	23		
8				2	22	67	89	47	
9				1	20	107	236	240	106
10				1	14	132	486	797	657
11					9	138	814	2 075	2 678
12					5	126	1 169	4 495	8 548
13					2	95	1 454	8 404	22 950
14					1	64	1 579	13 855	53 863
15					1	40	1 515	20 303	112 618
16						21	1 290	26 631	211 866
17						10	970	31 400	361 342
18						5	658	33 366	561 106
19						2	400	31 996	795 630
20						1	220	27 764	1 032 754
21						1	114	21 817	1 229 228
22							56	15 558	1 343 120
23							24	10 096	1 348 674
24							11	5 984	1 245 369
25							5	3 247	1 057 896
26							2	1 635	827 086
27							1	770	595 418
28							1	344	394 820
29								148	241 428
30								63	136 370
31								25	71 293
32								11	34 652
33								5	15 767
34								2	6 757
35								1	2 768
36								1	1 102
37									428
38									165
39									66
40									26
41									11
42									5
43									2
44									1
45									1
Sum	1	2	6	21	112	853	11 117	261 080	11 716 571

come identical under this operation are, by definition, isomorphic. As a final confirmation of our algorithm, the number of distinct (n,q) graphs was counted and compared with the predictions of Table I. Figure 1 summarizes the algorithm used in finding the most stable neutral and cation clusters having up to nine atoms.

One further complication should be noted. Although every possible Hückel structure for an n-atom cluster can be described by a simple graph, the converse of this statement is not true. In fact, atoms in the HMO model behave like hard spheres of radius r_0, and for two such atoms with position vectors $\mathbf{r}_i$ and $\mathbf{r}_j$, the following physical restriction is implied for all $1 \leqslant i \neq j \leqslant n$:

$$|\mathbf{r}_i - r_j| = 2r_0 \quad \text{if } H_{ij} = -1, \tag{10}$$

$$|\mathbf{r}_i - \mathbf{r}_j| > 2\mathbf{r}_0 \quad \text{if } H_{ij} = 0. \tag{11}$$

For some graphs, however, the conditions (10) and (11) cannot be fulfilled simultaneously. We refer to these graphs as geometrically forbidden graphs. Those for which the conditions (10) and (11) can rigorously hold or approximately hold we term allowed or nearly allowed graphs, respectively. Thus for each nominal Hückel structure, found to be particularly stable by the methods just outlined, it was also necessary to determine whether or not the graph was geometrically allowed. In the algorithm used in this work, we search for the position vectors $\mathbf{r}_i, i = 1,2,...,n$, which *maximize*, under the restriction of Eq. (10), the distances between nonbonded atoms i and j. If the resultant vectors do not satisfy Eq. (11), then the graph is not geometrically allowed. For this purpose, we define the "objective function"

$$S = \sum_{i<j} |\mathbf{r}_i - \mathbf{r}_j|^{-\gamma} \tag{12}$$

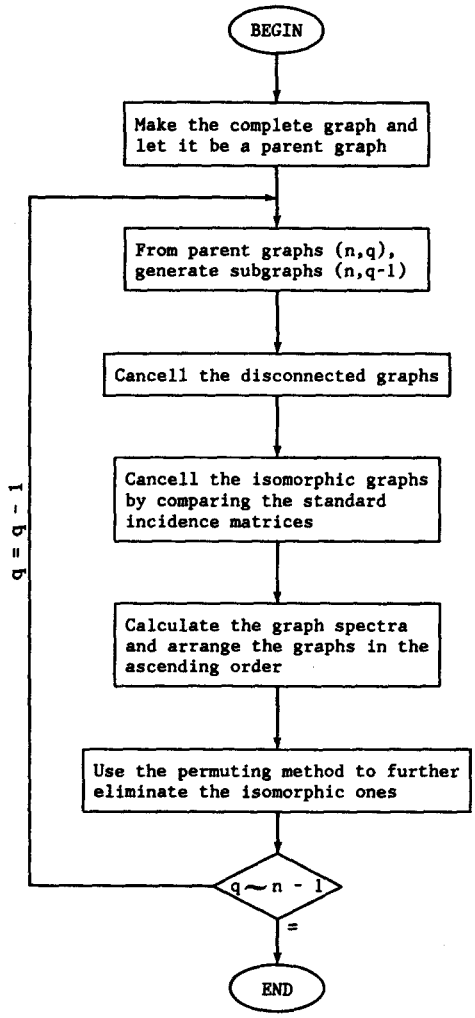

FIG. 1. Flow chart of the algorithm used to generate all simple connected graphs.

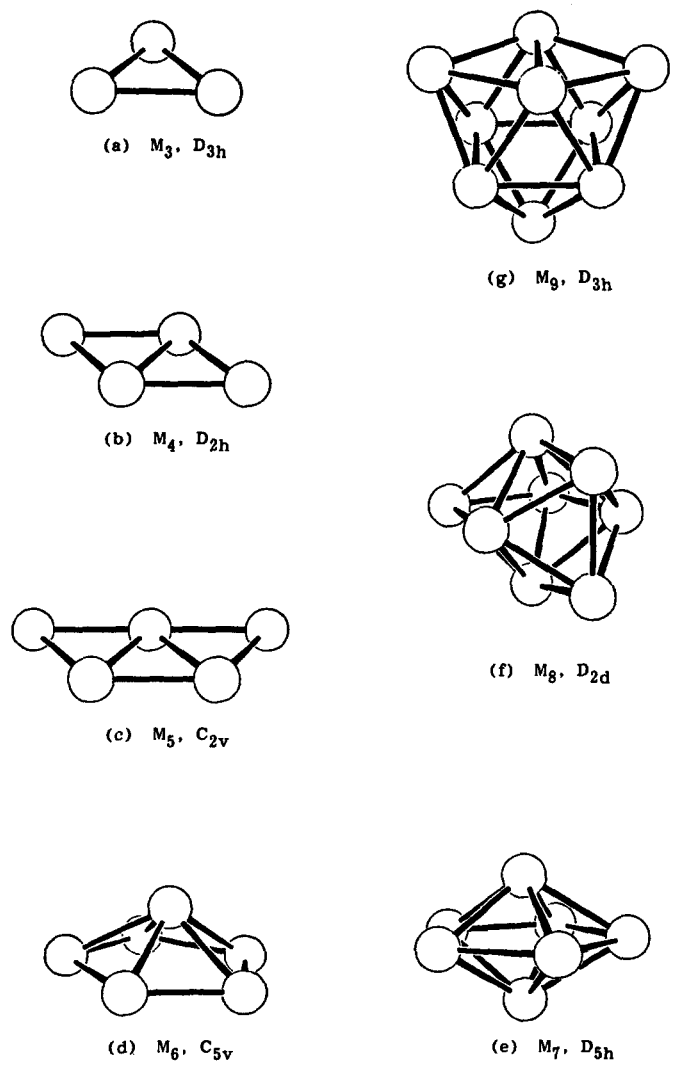

FIG. 2. Most stable structures for neutral metal clusters up to nine atoms.

and minimize it by using a constrained nonlinear optimization procedure[36] with the restriction of Eq. (10). In Eq. (12), the sum is over all $i<j$ for which $H_{ij}=0$, and the vectors $\mathbf{r}_i$ are in units of r_0. The exponent γ (here $\gamma=12$) was chosen to be as large as possible to ensure a rapid convergence without causing data overflow in the computation. In this way, the file of diagonalized graphs was searched in ascending energy order for allowed or nearly allowed structures. Some of the geometrical implications of this procedure are discussed in the following section.

III. RESULTS AND DISCUSSION

Figures 2 and 3 show the geometries found for the most stable Hückel neutral and cation clusters. Tables II and III give the corresponding binding energy [Eqs. (2) and (4)] in Hückel units (hu). Also included in the tables are the binding energy for the second most stable structures. The atomization energy of a neutral cluster, $\Delta E^0(n)$, is the energy change for the process

$$\mathrm{M}_n = n\mathrm{M}. \tag{13}$$

Thus

$$\Delta E^0(n) = n\alpha - E^0(n). \tag{14}$$

Similarly, for a cation cluster,

$$\mathrm{M}_n^+ = (n-1)\mathrm{M} + \mathrm{M}^+ \tag{15}$$

and

$$\Delta E^+(n) = (n-1)\alpha - E^+(n). \tag{16}$$

Table II and III give the atomization energy/atom, $\Delta E^0(n)/n$ and $\Delta E^+(n)/n$, for the neutral and cation species.

Table IV shows the *difference* between the atomization energy of the most stable and the second most stable Hückel structures expressed in both eV and Kelvin. For ease of comparison, it has been specialized to the case of sodium clusters using a value of $\beta = 0.38$ eV.[37] Interestingly, the energy difference does not become progressively smaller with increasing cluster size. Furthermore, the absolute magnitudes of these differences are quite large, suggesting that in most matrix isolation and cooled beam experiments, a single cluster geometry will predominate.

The geometries found for the second most stable neutral clusters, M_3–M_8, are, respectively: linear ($D_{\infty h}$), C_{2v} (e.g., see cluster 4.8 in Table I of Ref. 26), square pyramid (C_{4v}),

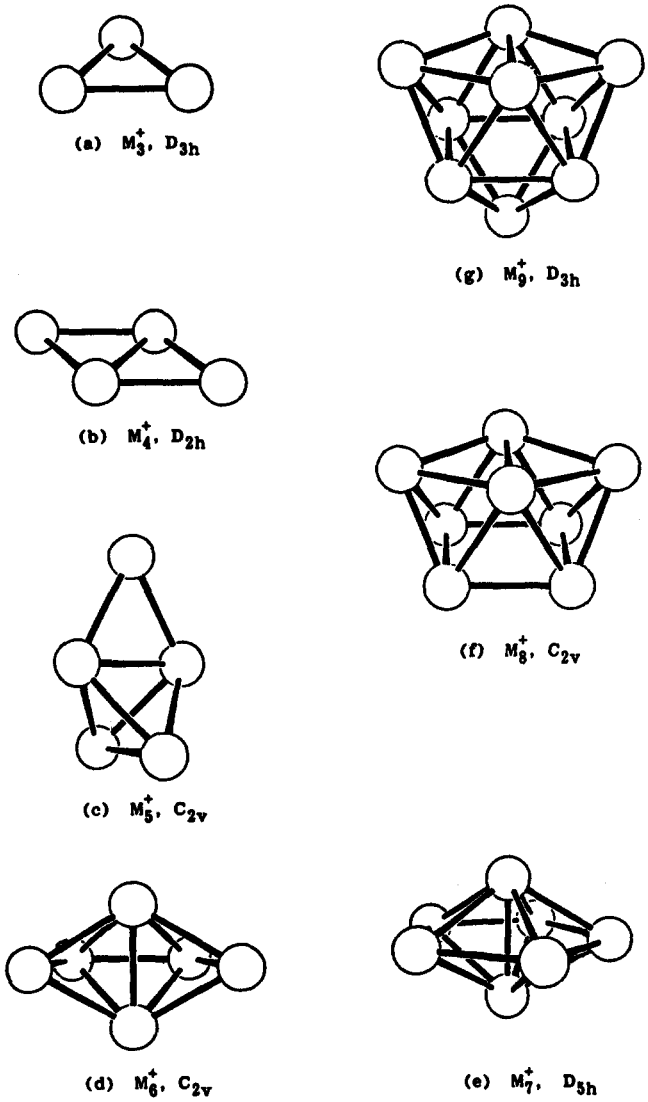

FIG. 3. Most stable structures for metal cluster cations up to nine atoms.

capped square pyramid (C_s), capped (but distorted) octahedron (C_s) and square antiprism (C_{2v}). The structures of the alkali hexamers deserve further comment. Our second most stable cluster (the capped square pyramid) is not the same as that found by local-spin-density calculations on Na_6.[27] The authors of Ref. 27 predict a D_{3h} hexamer to be approximately 0.04 eV less stable than the most stable C_{5v} structure. The HMO calculations find the D_{3h} and capped square pyramidal geometries to be nearly isoergic, but give 0.15 eV (Table IV of this paper) as the atomization energy difference between the two most stable Na_6 structures. In this context, it is interesting to note that appearance-potential data for gas-phase Na_6 show *two* breaks which differ in energy by 0.15 eV.[10] Accordingly, there is some ambiguity as to the exact ionization potential of Na_6.[7,10] The HMO data suggest that the threshold behavior of the hexamer could be attributed to the photoionization of at least two isomeric Na_6 species.

For all the neutral and cation species except M_8^+ and M_9, the most stable *allowed* HMO structures (Figs. 1 and 2 and Tables II and III) correspond to the most stable graphs [in the sense of Eqs. (2) and (4)]. For M_8^+, Eqs. (10) and (11) are not fulfilled for the most stable graph, and the true Hückel minimum [Fig. 2(f)] is, in fact, the second most stable graph. For M_9, the first 311 graphs are geometrically forbidden, and the D_{3h} structure shown in Fig. 1(g) pertains to the graph number 312. In the case of M_7^+ (but not the neutral heptamer), the geometry shown in Fig. 2(e) does correspond to the lowest energy graph but does not exactly fulfill the conditions (10) and (11). Thus for a pentagonal bipyramid composed of hard spheres, the two apical atoms

TABLE II. Binding energy and atomization energy/atom of the most stable and the second most stable neutral clusters.[a]

	First		Second	
n	$E^0(n)$	$\Delta E^0(n)/n$	$E^0(n)$	$\Delta E^0(n)/n$
1	0.0000	0.0000		
2	−2.0000	1.0000		
3	−3.0000	1.0000	−2.8284	0.9428
4	−5.1231	1.2808	−4.9624	1.2406
5	−6.6443	1.3289	−6.4721	1.2944
6	−9.3711	1.5619	−8.9786	1.4964
7	−11.1054	1.5865	−11.0692	1.5813
8	−14.1604	1.7701	−13.9969	1.7496
9	−15.6458	1.7384		

[a] Energy expressed in Hückel units (see the text).

TABLE III. Binding energy and atomization energy/atom of the most stable and the second most stable cation clusters.[a]

	First		Second	
n	$E^+(n)$	$\Delta E^+(n)/n$	$E^+(n)$	$\Delta E^+(n)/n$
1	0.0000	0.0000		
2	−1.0000	0.5000		
3	−4.0000	1.3333	−2.8284	0.9428
4	−5.1231	1.2808	−5.0000	1.2500
5	−7.3627	1.4725	−7.2915	1.4583
6	−9.0425	1.5071	−8.9786[b]	1.4964
7	−11.8753[b]	1.6965	−11.4949	1.6421
8	−13.7026	1.7128	−13.6712[b]	1.7089
9	−17.0600	1.8956	−16.8646	1.8738

[a] Energy expressed in Hückel units (see the text).
[b] These are nearly allowed structures (see the text).

TABLE IV. Difference in atomization energy between the most stable and the second most stable neutral sodium cluster structures.

	Atomization energy difference		
n	hu[a]	eV[b]	Kelvin
3	0.1716	0.065	760
4	0.1607	0.061	710
5	0.1722	0.065	760
6	0.3925	0.149	1730
7	0.0362	0.014	160
8	0.1635	0.062	720

[a] Data from Table II. hu ≡ Hückel unit.
[b] Using $\beta = 0.38$ eV (see Ref. 37).

cannot touch if the five ring atoms are in contact with their neighbors. However, the "gap" is so small that if we allow these spheres to soften a little bit, i.e., expand the five ring atoms a little (less than 1% of their diameters) and compress the two apical spheres a little, we end up with a nearly allowed geometry, which was taken to be the true Hückel minimum. The same argument is applied to the second most stable M_8^+. In this context, it is interesting to note that the local-spin-density calculations of Ref. 27 predict that Na_7 and Na_7^+ both have D_{5h} symmetry, but they find a significantly shorter apical–apical bond in the cation.

Experimentally, only the geometries of the alkali trimer and alkali septemer clusters are known with any certainty. ESR spectra[4,5] show that Li_7, Na_7, and K_7 have a pentagonal bipyramidal geometry. The alkali trimer molecules are best regarded as arising from a (static or dynamic) Jahn–Teller distortion of the equilateral triangle.[1–3] The subtleties of the Jahn–Teller effect are not, of course, incorporated in HMO theory but must be anticipated for those structures which have (at the simple Hückel level) orbitally degenerate ground states. Except in the case of the trimer and (see the paper following) M_{13} and M_{14}^+, the predicted HMO geometries are not orbitally degenerate. For M_3, *ab initio* calculations[20] find that the Jahn–Teller stabilization energy is only of the order of 10% of the total cluster atomization energy. For clusters larger than the trimer, Jahn–Teller energies would be expected to be proportionately less important.

A striking result of the HMO calculations is the excellent agreement between the most stable HMO structures and the equilibrium geometries predicted by recent *ab initio* (at least in comparison to simple Hückel) calculations. In particular, we refer to the pseudopotential local-spin-density (PP-LSD) calculations on Na_n and Na_n^+ ($n \leqslant 8$, $n = 13$) and the multireference diexcited configuration interaction (MRD-CI) results of Koutecký *et al.*[23–26] on M_4 and M_7 (M = Li, Na, K), Li_5, Li_6, and Li_{13}. For M_3–M_8, the most stable HMO geometry is exactly the same as that found by the two *ab initio* techniques. A similar result pertains to the SCF-LCAO-MO results of Rao *et al.*[38] for Li_3–Li_6. (We ignore the Jahn–Teller distortion of the trimer, *vide supra.*) For the cations, the HMO geometries for M_5^+ and M_6^+ are different from those of Ref. 27. The Hückel binding energy for the D_2 structure shown in Fig. 2 of Ref. 27 is -7.11 hu as compared to -7.36 hu for the geometry shown in Fig. 2(c) of this paper. For M_6^+, the geometry shown in Fig. 2 of Ref. 27 is our second most stable structure (see Table III). Except in the case of the trimer and rhombic tetramer, the Hückel and both the PP-LSD and MRD-CI geometries are quite different from the localized, diatomic-like structures found in Ref. 22. A comparison with the predictions of diatomics–in–molecule (DIM) calculations cannot easily be made, since the latter[21] omit several of the structures that both HMO and *ab initio* techniques found to be particularly stable. There is, however, a very good agreement as to the relative stabilities of differing cluster structures when similar geometries are compared using both HMO and DIM. This similarity has been previously noted for the case of the alkali pentamers.[4]

In conclusion, we reemphasize the close connection between HMO calculations and graph theory. For a given cluster size, the range of possible Hückel structures is fixed by the manifold of geometrically allowed graphs. The relative stability of a particular HMO structure is determined by the eigenvalue spectrum of its corresponding graph and so is independent of the (quantum or classical) mechanical details of the bonding. Accordingly, the Hückel minimum energy configuration is strongly related to the relative connectivity, i.e., topology of the cluster, at least in the case of the alkali metals.[39] We note that these simple and fundamental principles lead to structures and stabilities for small metal clusters that are in remarkable accord with the predictions of much more sophisticated computational techniques. In the following paper, we extend this comparison to include cluster binding energies and ionization potentials. We show that our quantum mechanical results include features of both the jellium and classical droplet models. In addition, we extrapolate from small cluster sizes to the bulk phase.

ACKNOWLEDGMENTS

Y.W. would like to thank Professor A. H. Stone for his beneficial discussion on graph theory, Dr. M. Hutchinson for his helpful discussions, and Professor W. D. Jones and Dr. T. Koritsanszky for their assistance in plotting the clusters. We are indebted to Professor A. W. Castleman, Jr. for bringing the photoionization data for Na_6 to our attention. TFG acknowledges support by the Office of Naval Research, the Air Force Office of Scientific Research (AFSC), United States Air Force, under Contract No. F49620-86-C-0009, and the National Science Foundation under Grant No. CHE-8519053. DML acknowledges support by the National Science Foundation under Grant No. CHE-8307164 and by the City University of New York PSC-BHE Faculty Research Award Program. The United States Government is authorized to reproduce and distribute reprints for governmental purposes notwithstanding any copyright notation hereon.

[1] D. M. Lindsay, D. R. Herschbach, and A. L. Kwiram, Mol. Phys. **32**, 1199 (1976).
[2] G. A. Thompson and D. M. Lindsay, J. Chem. Phys. **74**, 959 (1981).
[3] D. A. Garland and D. M. Lindsay, J. Chem. Phys. **78**, 2813 (1983).
[4] G. A. Thompson, F. Tischler, and D. M. Lindsay, J. Chem. Phys. **78**, 5946 (1983).
[5] D. A. Garland and D. M. Lindsay, J. Chem. Phys. **80**, 4761 (1984).
[6] (a) P. J. Foster, R. E. Leckenby, and E. J. Robbins, J. Phys. B **2**, 478 (1969); (b) E. J. Robbins, R. E. Leckenby, and D. Willis, Adv. Phys. **16**, 739 (1967).
[7] A. Hermann, E. Schumacher, and L. Woste, J. Chem. Phys. **68**, 2327 (1978).
[8] M. M. Kappes, P. Radi, M. Schär, and E. Schumacher, Chem. Phys. Lett. **119**, 11 (1985).
[9] M. M. Kappes, M. Schär, P. Radi, and E. Schumacher, J. Chem. Phys. **84**, 1863 (1986).
[10] K. I. Peterson, P. D. Dao, R. W. Farley, and A. W. Castleman, Jr., J. Chem. Phys. **80**, 1780 (1984).
[11] W. A. Saunders, K. Clemenger, W. A. de Heer, and W. D. Knight, Phys. Rev. B **32**, 1366 (1985).
[12] W. D. Knight, K. Clemenger, W. A. de Heer, W. A. Saunders, M. Y. Chou, and M. L. Cohen, Phys. Rev. Lett. **52**, 2141 (1984).
[13] W. D. Knight, W. A. de Heer, and K. Clemenger, Solid State Commun. **53**, 445 (1985).

[14]K. P. Huber and G. Herzberg, *Constants of Diatomic Molecules* (Van Nostrand, New York, 1979).
[15]C. H. Wu, J. Chem. Phys. **65**, 3181 (1976).
[16]C. H. Wu, J. Phys. Chem. **87**, 1538 (1983).
[17]K. Hilpert, Ber. Bunsenges. Phys. Chem. **88**, 260 (1984).
[18]For a summary of the earlier alkali trimer calculations see: E. R. Dietz, Phys. Rev. A **23**, 751 (1981).
[19]J. L. Martins, R. Car, and J. Buttet, J. Chem. Phys. **78**, 5646 (1983).
[20]T. C. Thompson, G. Izmirlian, S. J. Lemon, D. G. Truhlar, and C. A. Mead, J. Chem. Phys. **82**, 5597 (1985).
[21]S. C. Richtsmeier, D. A. Dixon, and J. L. Gole, J. Phys. Chem. **86**, 3942 (1982).
[22]J. Flad, H. Stoll, and H. Preuss, J. Chem. Phys. **71**, 3042 (1979).
[23]H.-O. Beckmann, J. Koutecký, and V. Bonacić-Koutecký, J. Chem. Phys. **73**, 5182 (1980); D. Plavsić, J. Koutecký, G. Pacchioni, and V. Bonacić-Koutecký, J. Phys Chem. **87**, 1096 (1983).
[24]G. Pacchioni, D. Plavsić, and J. Koutecký, Ber. Bunsenges. Phys. Chem. **87**, 503 (1983).
[25]P. Fantucci, J. Koutecký, and G. Pacchioni, J. Chem. Phys. **80**, 325 (1984).
[26]J. Koutecký and P. Fantucci, Chem. Rev. **86**, 539 (1986).
[27]J. L. Martins, J. Buttet, and R. Car, Phys. Rev. B **31**, 1804 (1985).
[28]E. Hückel, Z. Phys. **70**, 204 (1931); **72**, 310 (1932); **76**, 628 (1932).
[29]L. Salem, *Molecular Orbital Theory of Conjugated Systems* (Benjamin, New York, 1966).
[30]A. Streitwieser, *Molecular Orbital Theory* (Wiley, New York, 1961).
[31]F. Harary, *Graph Theory* (Addision–Wesley, Massachusetts, 1969).
[32]The close connection between Hückel theory and the topology of conjugated molecules has long been recognized. See, for example, N. Trinajstic, in *Semiempirical Methods of Electronic Structure Calculations, Part A: Techniques*, edited by G. A. Segal (Plenum, New York, 1977).
[33]F. Harary and E. M. Palmer, *Graphical Enumeration* (Academic, New York, 1973).
[34]D. G. Corneil and C. C. Gotlieb, J. Assoc. Comput. Mach. **17**, 51 (1970).
[35]In some graphs, however, it is possible that several vertices may have exactly the same connectivity, for example, the symmetric points in a graph. Thus, starting from different incidence matrices, we may end up with different S_q, even if they represent intrinsically the same graph. In order to get a unique standard incidence matrix, we interchange these vertices, thus generating several possible S_q which represent the same graph. For two such S_q, we compare, term by term and, in order of increasing i, their b_i elements. When two b_i are found to be different, we choose that S_q which has the larger value of b_i. In this way, we select the optimized sequence order vector.
[36]D. M. Himmelblau, *Applied Nonlinear Programming* (McGraw–Hill, New York, 1972).
[37]D. M. Lindsay, Y. Wang, and T. F. George, J. Chem. Phys. **86**, 3500 (1986).
[38]B. K. Rao and P. Jena, Phys. Rev. B **32**, 2058 (1985); B. K. Rao, S. N. Khanna, and P. Jena, Solid State Commun. **56**, 731 (1985).
[39]It is interesting that recent calculations for Si and Ge clusters also predict structures similar in many cases to those of the alkali metals. See D. Tománek and M. A. Schlüter, Phys. Rev. Lett. **56**, 1055 (1986); and G. Pacchioni and J. Koutecký, J. Chem. Phys. **84**, 3301 (1986).